Abdominal Radiology (2019) 44:3843–3857
https://doi.org/10.1007/s00261-019-02168-z

SPECIAL SECTION: UROTHELIAL DISEASE

Preoperative imaging for locoregional staging of bladder cancer

S. Mojdeh Mirmomen[1] · Atul B. Shinagare[2,3] · Kristin E. Williams[2,3] · Stuart G. Silverman[3] · Ashkan A. Malayeri[1,3]

Published online: 3 August 2019

Abstract
Bladder cancer is the ninth most common cancer, expected to lead to an estimated 17,670 deaths in the United States in 2019. Clinical management and prognosis of bladder cancer mainly depend on the extent of locoregional disease, particularly whether bladder muscle is involved. Therefore, bladder cancer is often divided into superficial, non-muscle-invasive bladder cancer and muscle-invasive bladder cancer; the latter often prompts consideration for cystectomy. While precise staging prior to cystectomy is crucial, the optimal preoperative imaging modality used to stage the disease remains controversial. Transurethral resection of bladder tumor (TURBT) followed by computed tomography (CT) urography is the current recommended approach for staging bladder cancer but suffers from a high rate of understaging. We review the recent literature and compare different imaging modalities for assessing the presence of muscle invasion and lymph node involvement prior to cystectomy and highlight the advantages of each modality.

Keywords Bladder cancer staging · Preoperative imaging modality · Computed tomography · Magnetic resonance imaging · Positron emission tomography

Introduction

Bladder cancer is the most common urothelial malignancy [1, 2]. It is the ninth most common cancer overall with an estimated 80,470 new cases (61,700 among males and 18,770 among females) and 17,670 deaths (12,870 among males and 4,800 among females) in the US in 2019 [1, 2]. Men are approximately three times more likely than women to be diagnosed with bladder cancer; patients are usually diagnosed in the 8th decade of life [3]. Painless hematuria and frequency of urination are the most common symptoms; urinary tract obstruction and pain are limited to advanced cases. Patients with symptoms of bladder cancer are typically evaluated with computed tomography (CT) urography and cystoscopy, and when a suspected lesion is found, transurethral resection of the bladder tumor (TURBT) to both verify the diagnosis and stage the disease. Clinical management and prognosis depend in large part on the presence of disease within bladder muscle—muscle-invasive bladder cancer (MIBC) versus superficial, non-muscle-invasive bladder cancer (non-MIBC)—and the presence of nodal and metastatic lesions [2, 3].

Approximately 75–85% of patients with bladder cancer present with non-muscle-invasive disease (Ta, T1 or Tis), which is typically treated with bladder-sparing techniques such as TURBT alone with or without adjuvant intravesical or systemic therapies [4]. MIBC (≥ T2 disease) is commonly treated with partial or radical cystectomy with pelvic lymph node dissection, neoadjuvant or adjuvant chemotherapy and radiation [2, 3, 5]. The detection of MIBC is important due to significant differences in outcome and treatment strategies. Currently, TURBT is the method of choice to detect muscle invasion, however, several studies have indicated that this method may understage the disease in up to 40% of patients [6, 7]. Therefore, a noninvasive alternative for accurate staging of the bladder cancer would be of immense value.

The Tumor, Node, Metastasis (TNM) system is currently the standard staging system used by the American Joint Committee on Cancer (AJCC) for bladder cancer (Table 1) [8]. Given the suboptimal performance of TURBT in local staging of the bladder cancer, several noninvasive

✉ Ashkan A. Malayeri
ashkan.malayeri@nih.gov

[1] Radiology and Imaging Sciences, Clinical Center, National Institutes of Health, Bethesda, MD, USA

[2] Dana-Farber Cancer Institute, Boston, MA, USA

[3] Department of Radiology, Brigham and Women's Hospital, 75 Francis Street, Boston, MA, USA

Table 1 Bladder cancer TNM staging system adapted from the American Joint Committee on Cancer (AJCC) 8th edition [8]

TNM stage	T	N	M	Description
0a	Ta	N0	M0	Ta defined as noninvasive papillary carcinoma; N0 defined as no lymph node involvement; M0 defined as no distant metastasis
0is	Tis	N0	M0	Tis defined as urothelial carcinoma in situ: 'flat tumor'
I	T1	N0	M0	T1 defined as tumor invasion into the subepithelial connective tissue (lamina propria)
II	T2a	N0	M0	T2a defined as tumor invasion into the inner half of the detrusor muscle
	T2b	N0	M0	T2b defined as tumor invasion into the outer half of the detrusor muscle
IIIA	T3a	N0	M0	T3a defined as tumor invasion into the perivesical tissue microscopically
	T3b	N0	M0	T3b defined as tumor invasion into the perivesical tissue macroscopically
	T4a	N0	M0	T4a defined as tumor invasion into the adjacent organs (prostatic stroma, seminal vesicles, uterus, vagina)
	T1- T4a	N1	M0	N1 defined as single regional lymph node metastasis in the true pelvis (perivesical, obturator, internal and external iliac, or sacral lymph node)
IIIB	T1- T4a	N2, N3	M0	N2 defined as multiple regional lymph node metastasis in the true pelvis (perivesical, obturator, internal and external iliac, or sacral lymph node metastasis); N3 defined as lymph node metastasis to the common iliac lymph nodes
IVA	T4b	Any N	M0	T4b defined as tumor invasion into the pelvic side wall or abdominal wall
	Any T	Any N	M1a	M1a defined as distant metastasis limited to lymph nodes beyond the common iliac chains
IVB	Any T	Any N	M1b	M1b defined as distant metastasis to site(s) other than lymph nodes

morphological and functional imaging-based methods have been proposed that can improve the accuracy of local staging of the bladder cancer [9]. Nodal staging with conventional cross-sectional imaging [CT and magnetic resonance imaging (MRI)] is based on lymph node size, which often leads to understaging of metastatic disease to locoregional lymph nodes in up to 30% [10]. This review highlights the advantages and disadvantages of preoperative imaging studies for locoregional staging of bladder cancer, including the local staging and adjacent nodal involvement.

Imaging modalities

Computed tomography (CT)

CT urography is the most widely used imaging modality for detection and staging of urothelial carcinoma with a reported diagnostic accuracy of 91% in detection and 35–55% in staging [11, 12]. At our institution, CT urography is performed as a three-phase examination that includes non-contrast, urothelial and excretory phases. Some institutions use a split-bolus technique, in which images in the urothelial and excretory phases are obtained at the same time with different injection times. This two-phase examination reduces scanning time and radiation dose, however, there is some evidence that contrast material used in the excretory phase can mask small lesions and limit the evaluation of tumor enhancement during a dedicated urothelial phase [13]. In a retrospective evaluation of 2600 patients with hematuria, Sadow et al. showed that CT urography can be used to detect bladder cancer; while the negative predictive value was 98%, the sensitivity was 79% [12] (Fig. 1). Although CT has restrictions in accurately differentiating between T1, T2 and T3a due to its inability to individually identify layers of the bladder wall, it may provide useful staging information regarding perivesical invasion of high-grade T3b and T4 tumors [13, 14] (Fig. 2). Several groups have investigated the role of CT in local staging of bladder cancer, for example Caterino et al. utilized three different CT techniques; imaging the bladder filled with urine, intravenous contrast material or air. In their study, patients were assigned to four groups; Ta–T1 (group I), T2–T3a (group II), T3b (group III) and T4 (group IV). Their results showed that the air-insufflated bladder technique had the highest accuracy in evaluating the degree of mural invasion in the first three groups. The accuracy of all techniques were the same (100%) in characterizing advanced tumors with adjacent organ invasion (T4) [15]. We summarize the results of CT-based studies for local staging of bladder cancer in Table 2; Overall, CT is modestly accurate in the detection of perivesicular invasion ($\geq$T3), ranging from 49 to 93%.

Identifying lymph node involvement on CT is usually based on lymph node size and shape. Lymph nodes are considered abnormal on imaging if the short axis diameter is greater than 8 and 10 mm in pelvis and abdomen, respectively [16]. This may lead to missing metastatic disease in lymph nodes smaller than 8 mm in short axis diameter, while over-diagnosing the metastatic involvement in reactive lymph nodes larger than 10 mm in short axis diameter in up to 30% of the patients [10]. Pichler et al. demonstrated that the best cutoff value for metastatic pelvic lymph node identification was 8 mm (sensitivity and specificity of 45.5% and 91.5%), Li et al. suggested that 6.8 mm is the optimal short

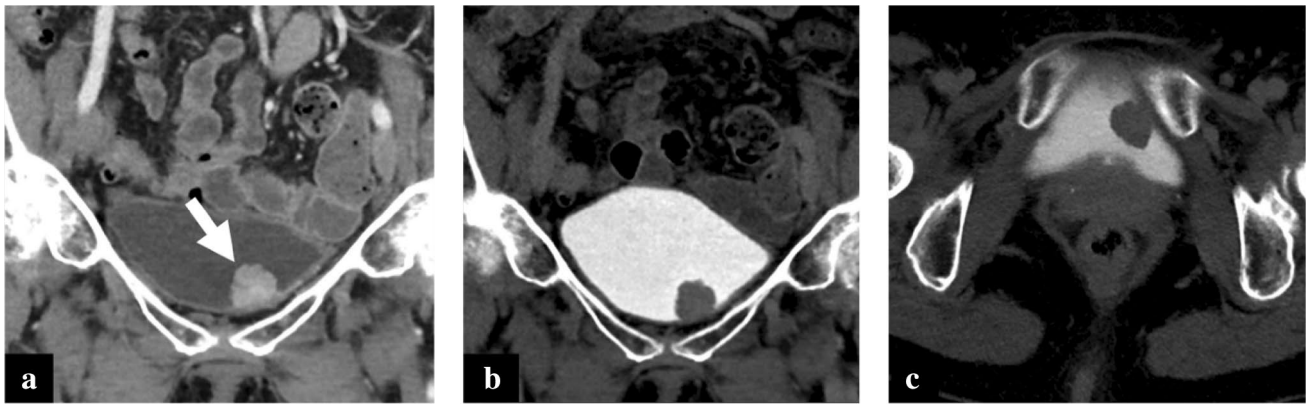

Fig. 1 75-year-old woman with microscopic hematuria. At CT urography, a 1.9 cm papillary mass arises from the left bladder wall (arrow). The uninterrupted adjacent wall and lack of findings in the perivesical fat suggests the tumor is organ confined (≤T3). These findings were concordant with results from TURBT

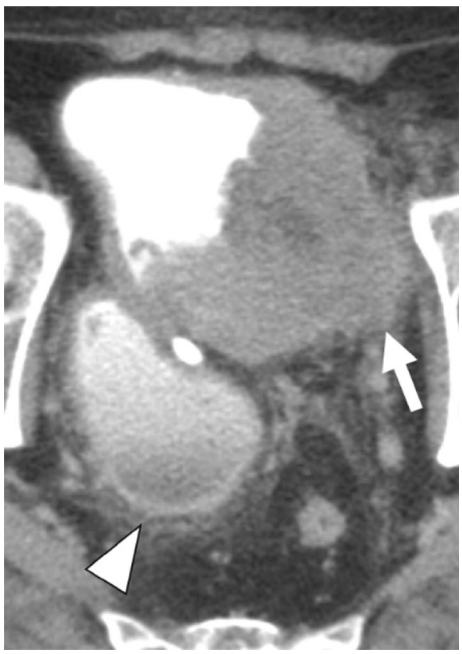

Fig. 2 67-year-old man with gross hematuria. CT urogram demonstrates a 7.8 cm mass arising from the left lateral bladder wall. Perivesical stranding and nodularity suggests extravesicular extension of tumor (≥T3) (arrow). Large diverticulum arises from the right posterolateral bladder wall (arrowhead). Extravesicular extension of tumor was confirmed at surgery, with involvement of the rectosigmoid (T4)

axis diameter cutoff (area under the ROC curve: 0.815) [16, 17]. These studies showed that the sensitivity of CT images in detecting nodal metastases is strictly related to the size of the involved lymph node and reducing the size threshold can cause a high false-negative results. Lymph node size is important both for the diagnose of metastatic lymph nodes, and as an indicator of prognosis in patients with bladder cancer. In a study of 206 patients, Schmid et al. reported that when metastatic pelvic lymph nodes are greater than 5 mm in diameter, the risk of death due to bladder cancer significantly increases [18]. We summarize the results of CT-based studies in Table 2; overall, the performance of CT for diagnosis of lymph node metastasis is variable amongst different studies, ranging from 54 to 86%.

Even though CT cannot be used to precisely stage bladder cancer due to moderate accuracy in differentiating MIBC from superficial, non-MIBC and highly variable results for the diagnosis of metastatic lymph nodes, it remains the mainstay for initial staging of bladder cancer because of its cost-effectiveness, availability, and utility in detecting both metastatic disease in the entire abdomen and pelvis and when a CT urography protocol is used, synchronous upper tract cancers.

Magnetic resonance imaging (MRI)

Magnetic resonance (MR) urography provides valuable information on bladder and the synchronous upper urinary tract disease. In comparison to CT urography, MR urography has shown a lower sensitivity in detecting upper tract disease (67% vs 88–100%), however, it remains an alternative to CT urography in patients with contraindications to CT [32]. For local T staging of bladder cancer, MRI is superior to CT due to its high soft tissue contrast resolution [33]. The added value of MRI is in part due to the functional data derived from diffusion-weighted imaging (DWI) and dynamic contrast enhanced (DCE) imaging, which can provide additional information regarding tumor invasion, especially in differentiating superficial from muscle-invasive tumors [3, 34, 35]. Although new MRI sequences may improve our ability to further improve nodal staging, MRI and CT have been shown to perform similarly because nodal involvement is

Table 2 Sensitivity, specificity and accuracy for detection of perivesicular invasion (≥T3) and lymph node involvement with CT

Author/[Ref]	Year	Study type	Number of patients	Imaging modality	Perivesicular invasion (≥T3)			Lymph node metastasis		
					Sensitivity (%)	Specificity (%)	Accuracy (%)	Sensitivity (%)	Specificity (%)	Accuracy (%)
Kim/ [19]	2004	Prospective	67	CECT	89	95	93	67		
Baltaci/ [20]	2008	Retrospective	100	CT	85	63	72	31	94	86
Lodde/ [21]	2010	Prospective	70	CECT				33	100	
Swinnen/ [22]	2010	Prospective	51	CT				46	92	80
Maurer/ [23]	2011	Prospective	44	CECT				75	56	61
Hitier-Berthsult/ [24]	2012	Prospective	52	CECT				9	90	56
Tritschler/ [25]	2012	Retrospective	276	CT	62		49			54
Nayak/ [26]	2013	Prospective	25	CECT				44		
Goodfellow/ [27]	2014	Retrospective	93	CT				46	98	83
Aljabery/ [28]	2015	Retrospective	54	CECT				41	89	
Jeong/ [29]	2015	Prospective	61	CECT				29	98	
Horn/ [30]	2015	Retrospective	231	CECT				53	94	83
Oz/ [31]	2016	Retrospective	26	CECT	83	100	83	36	92	
Pichler/ [16]	2017	Retrospective	70	CECT				27[a]	97	86
								45.5[b]	91.5	84
								54.5[c]	85	80
Li/ [17]	2018	Retrospective	191	CECT				83[d]	64	

CT computed tomography, *CECT* contrast-enhanced computed tomography

[a]Pelvic lymph node is considered positive, if the largest short axis diameter was > 10 mm

[b]Pelvic lymph node is considered positive, if the largest short axis diameter was > 8 mm

[c]Pelvic lymph node involvement was defined based on the subjective assessment

[d]Pelvic lymph node is considered positive, if the largest short axis diameter was > 6.8 mm

based on morphological patterns in both [3, 36]. Each individual sequence used when performing an MRI of the pelvis (or MR urography) is discussed with respect to both findings and contribution to staging.

T2-weighted imaging (T2WI)

T2WI is the mainstay of bladder cancer staging as it depicts individual layers of the bladder wall and their relationship to the tumor (Fig. 3). Superficial, non-MIBC appears as an intermediate to high-signal intensity mass on T2WI with an intact adjacent hypointense detrusor muscle. In contrast, muscle-invasive tumors interrupt the detrusor muscle [37] (Fig. 4).

Diffusion-weighted imaging (DWI)

DWI relies on detection of Brownian motion of free-water molecules. Tumors with high cell density typically lead to restricted diffusion of water molecules and show high-signal intensity on DWI. The apparent diffusion coefficient (ADC) map is a quantitative display of the degree of restricted water diffusion. An ADC value can also be derived; its value decreases as tumor aggressiveness increases [38, 39]. DWI has shown promise in both detection and staging bladder tumors as well as detecting lymph node involvement [40] (Fig. 5). In comparison to T2WI alone, studies have reported superior sensitivity, specificity and accuracy when both T2WI and DWI were used to differentiate superficial from invasive tumors [39, 40]. Wu et al. showed that the diagnostic performance of combined DWI and T2WI was more accurate than DWI alone, especially in differentiating Tis -T1 from ≥ T2 disease [41].

In a study of 36 bladder cancer patients by Papalia et al., involved lymph nodes demonstrated diffusion restriction manifested as high-signal intensity on DWI with a b value of 1000 s/mm^2 and low-signal intensity on ADC map. The ADC value of 0.86×10^{-3} mm^3/s or less was considered to be malignant with sensitivity of 76.4% and specificity of 89.4% in this study [36].

Dynamic contrast-enhanced (DCE) imaging

DCE imaging is used to detect tumor based on tumor angiogenesis. Hypervascular malignant lesions exhibit early enhancement on DCE images [42–44] (Fig. 6). Several studies have shown relative accuracies of DCE imaging in differentiating superficial and muscle-invasive tumors as well as between organ-confined and non-organ-confined tumors, ranging from 85–97% to 82–84%, respectively [35, 42]. Gupta et al. showed that both DCE imaging and DWI performed similarly when staging locally advanced T4 tumors with sensitivity of 100%, and specificity and accuracy of more than 96%, however, the performance of both techniques was significantly reduced in tumors of lower stages. The diagnostic accuracy of DWI in

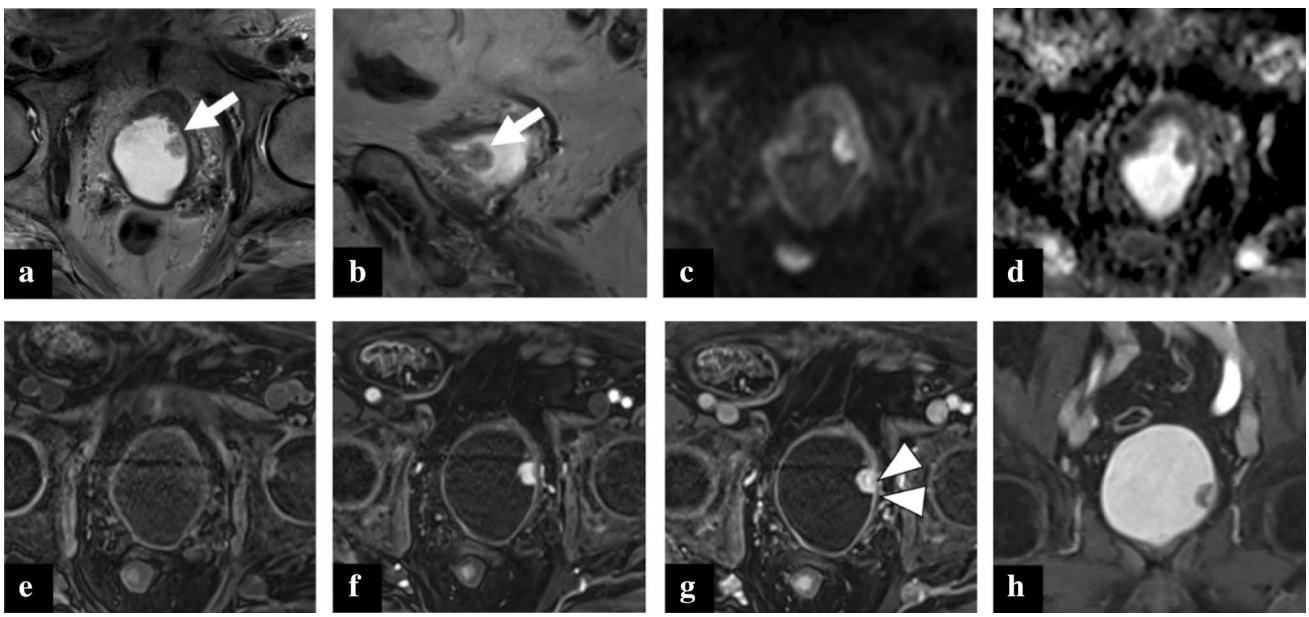

Fig. 3 81-year-old man with distant history of bladder cancer presents with hematuria. MR urogram demonstrates a 1.5 cm T2 hyperintense papillary mass with a stalk (arrow) (**a** and **b**). The mass demonstrates restricted diffusion on high b value DWI that was confirmed on ADC (**c** and **d**). Four-phase DCE images demonstrate avid enhancement with thickened subjacent inner layer of the bladder wall (arrow heads) (**e**–**h**). Surgery was consistent with high-grade T1 TCC

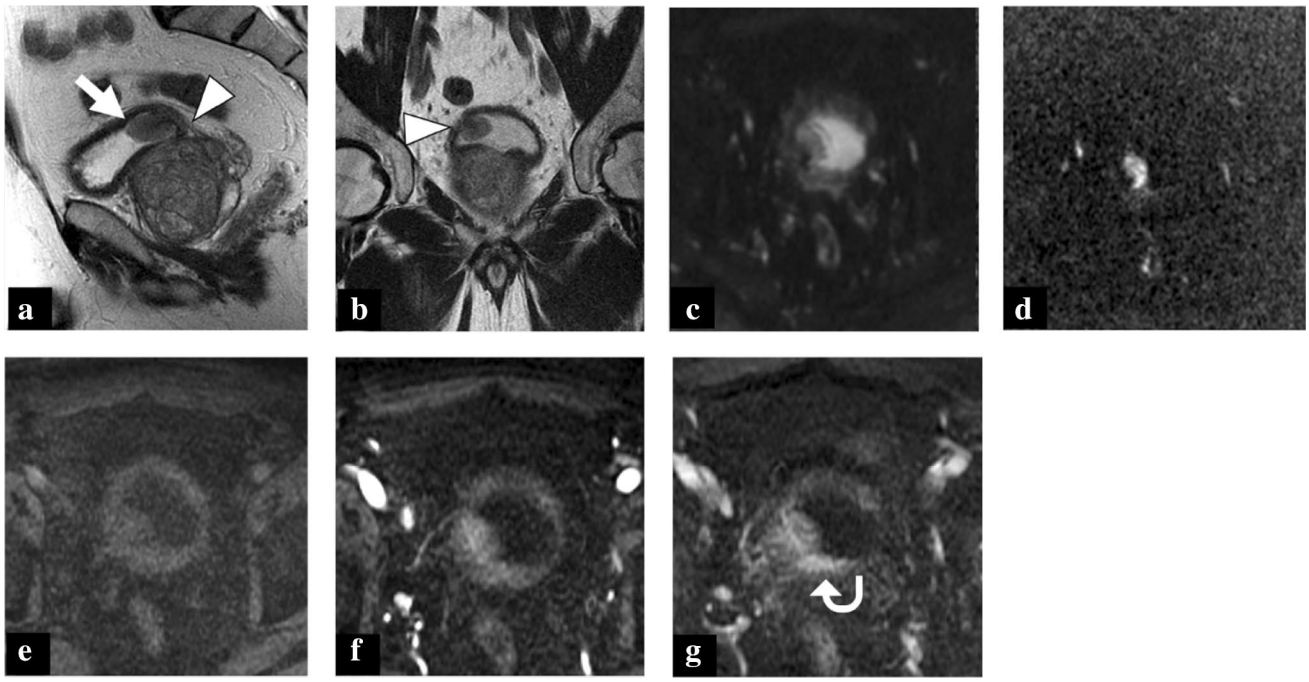

Fig. 4 75-year-old man with hematuria was found to have a polypoid bladder mass on MR urogram. The mass (arrow) at the posterior bladder wall demonstrates T2 hyperintensity on sagittal (**a**) and coronal (**b**) T2 weighted images. There is increased T2 signal within the subjacent bladder wall (arrowheads). However, there is no evidence of extension of the mass beyond the bladder wall. The mass demonstrates restricted diffusion on low and high b-value images (**c** and **d**). The mass is isointense to the bladder wall on precontrast T1-weighted images (**e**) and demonstrates enhancement after injection of contrast (**f** and **g**). Note enhancement deep into the muscular layer as demonstrated on post contrast images (curved arrow) consistent with pathologic staging of T2b

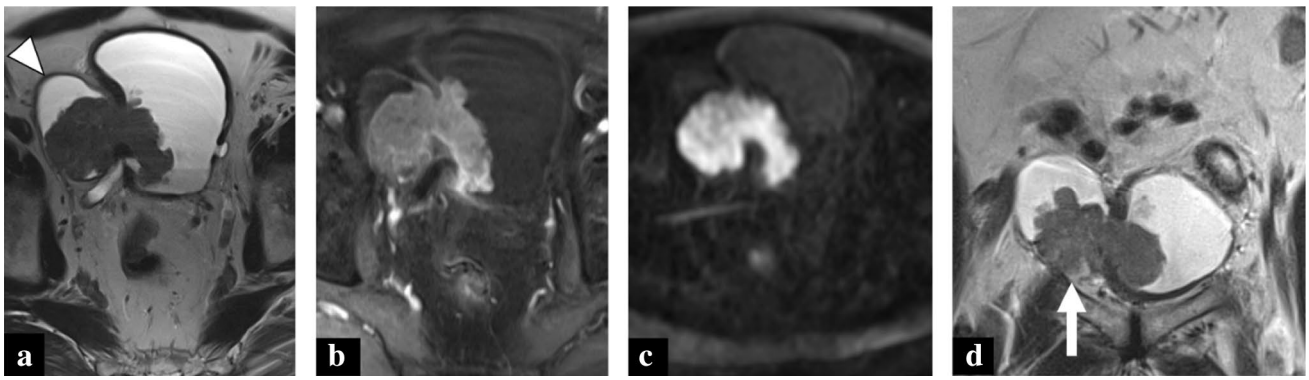

Fig. 5 78-year-old man with painless hematuria. MR urogram T2WI (**a**) demonstrates a 6.0 cm mass along the right bladder base, with extension into a large right posterolateral bladder wall diverticulum (arrowhead). The mass demonstrates heterogenous enhancement (**b**) and marked restricted diffusion (**c**). Invasion of the perivesical (T3) adipose tissue (arrow) was demonstrated only on coronal images (**d**) and was confirmed at surgery

differentiating organ-confined from non-organ-confined tumors was higher than DCE imaging in this study but results were better when both were used in combination. Therefore, the authors recommended a combination of DWI and DCE imaging for preoperative staging of bladder cancer [44]. This study and several others have demonstrated the superiority of multiparametric MRI (mpMRI), in which a combination of anatomic (T2WI and DCE) and functional imaging such as DWI, diffusion tensor imaging (DTI) and perfusion-weighted imaging (PWI) were used for staging bladder cancer [37]. Panebianco et al. demonstrated that a comprehensive mpMRI protocol with a combination of T2WI, PWI, DWI, and DTI outperformed other combinations of MRI sequences for the diagnosis of

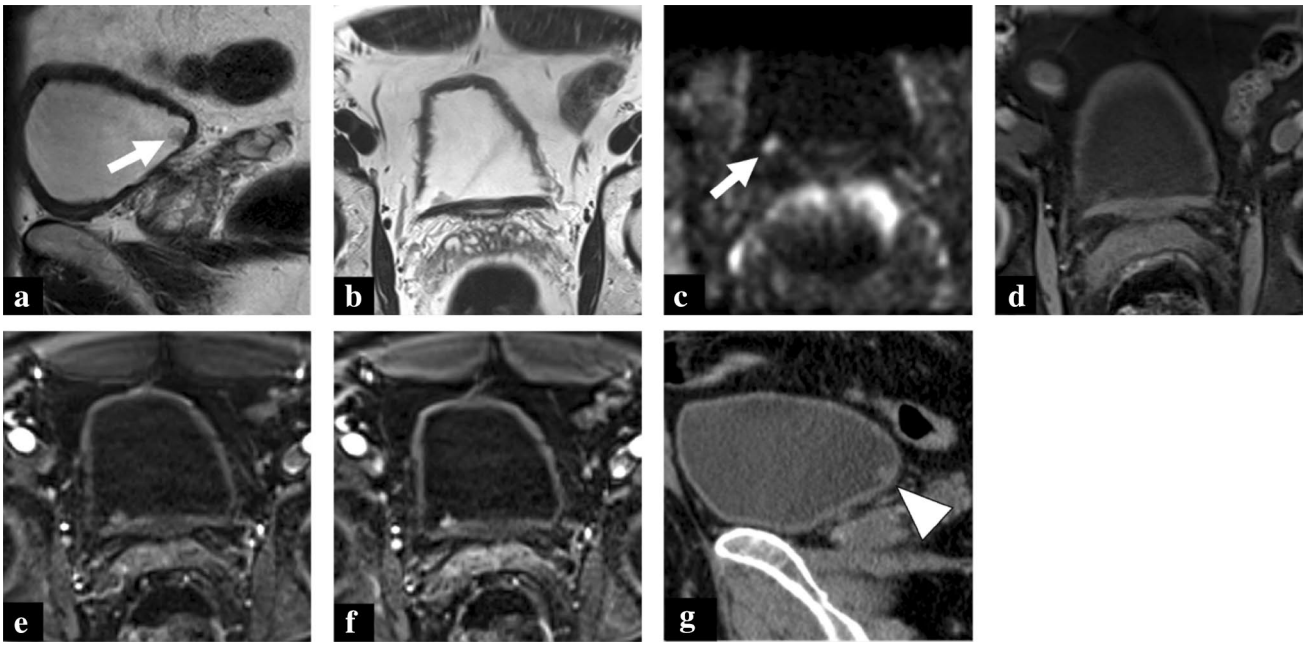

Fig. 6 62-year-old man with incidentally detected bladder mass on prostate MRI. The mass demonstrates T2 hyperintensity and is confined to the mucosal surface (**a** and **b**) with restricted diffusion as seen on high b-value image (arrow) (**c**). DCE images demonstrate avid enhancement of the mass with no interruption of the subjacent bladder wall. TURBT was performed and the mass was shown to be grade 1 TCC and staged as Ta. Staging CT demonstrated the mass (arrowhead), however, the distinction of the mass and the adjacent wall was impossible on CT (**g**)

muscle-invasive bladder cancer (AUC: 0.992) [33]. We summarize the results of MRI-based studies in differentiating superficial versus muscle-invasive bladder cancer in Table 3 and organ-confined versus locally advanced tumors in Table 4.

Ultra-small superparamagnetic particles of iron oxide (USPIO) enhanced-MRI

There are several alternatives to conventional gadolinium-based contrast agents. One of these agents is USPIO [45]. When injected, USPIO is a lymphotropic iron oxide agent that is absorbed by normal macrophages within lymph nodes. Normal lymph nodes absorb the agent, and therefore, show a signal intensity loss of more than 15% on T2WI due to iron-induced magnetic susceptibility. Lymph nodes replace with tumor do not contain macrophages, therefore do not take up the agent and show no signal loss on the same sequence [45, 46]. In a study of 75 patients with either bladder or prostate cancer, preoperative evaluation of lymph nodes with (USPIO)-enhanced MRI showed sensitivity, specificity and accuracy of 58.3, 83 and 76.4, respectively [46]. Another study on the same population reported improved detection rate of metastatic lymph nodes on combined USPIO-DW-MRI with a median time spent of 9 min for reading pelvic MRI in comparison to 32 min with USPIO-MR alone since benign lymph nodes are not displayed on USPIO-DWI and the need for the node to node comparison between pre and post contrast sequences was obviated [47]. We summarize the results of studies on the role of MRI in differentiating metastatic lymph nodes in Table 5.

Positron emission tomography (PET)

[18F] fluoro-D-glucose (18F-FDG) PET scan is the most common molecular imaging technique for preoperative staging of various malignancies, however, there are some limitations in the evaluation of bladder cancer. As an analog of glucose, 18 F-FDG is excreted in the urine, and therefore, accumulates in the bladder. As a result, the detection of bladder masses can be challenging when there is a high level of activity in the bladder (Fig. 7). Administration of oral hydration and forced diuresis by an intravenous diuretic, bladder catheterization with irrigation, and utilization of different radiotracers are methods applied to overcome this limitation [55–57]. Forced diuresis with oral hydration method has been shown to be the safest method to induce accelerated excretion of urinary radioactivity, providing high-resolution images [56].

In addition to the role of PET-CT in locoregional staging, this modality can help in establishing the prognosis. Drieskens et al. reported a median survival of 13.5 months in patients with positive nodal and distant metastasis on PET-CT scans, and 32 months when the scans were negative for metastasis using the Kaplan–Meier survival curves [58]. To evaluate the clinical utility of PET-CT in patients with

Table 3 MRI characteristics in differentiating of superficial (Ta, T1) from muscle-invasive bladder cancer (T2, T3, T4)

Author/[Ref]	Year	Study type	Number of patients	MRI sequence	Superficial vs. muscle invasive		
					Sensitivity (%)	Specificity (%)	Accuracy (%)
Tekes/ [35]	2005	Retrospective	71	Contrast enhanced images	95–97	55–67	76–83
Takeuchi/ [40]	2009	Prospective	40	T2 WI	88	74	79
				T2 WI + DWI	88	100	96
				T2 WI + contrast enhanced images	94	86	88
				All sequences	94	100	98
Rajesh/ [48]	2011	Retrospective	100	T1WI/T2WI/contrast enhanced images	78	93	85
Ghafoori/ [49]	2012	Prospective	86	T1WI/T2WI/contrast enhanced images	98	82	
Wu/ [41]	2013	Prospective	362	T2WI	81–91	71–79	74–83
				DWI	86–91	88-92	87–92
				T2WI + DWI	89–94	93-100	92–98
Sevcenco/ [38]	2014	Prospective	51	DWI (ADC)	90	79	
Gupta/ [44]	2014	Retrospective	60	DCE imaging	62.5	100	90
				DWI	62.5	100	90
Rabie/ [42]	2016	Prospective	45	DCE imaging	97	100	97
Zytoon/ [50]	2016	Prospective	50	Contrast enhanced images	92	100	94
				Contrast enhanced images + DWI	100	80	97
Barsoum/ [39]	2017	Prospective	50	T2WI	97	64	88
				DWI	100	86	96
				T2WI + DWI	100	86	96
Lee/ [51]	2017	Retrospective	62	T2WI	50	56	53
				DWI	58	78	69
				T2WI + DWI	65	81	74
				Fused DWI and T2WI (Fusion MRI)	81	78	79
Panebianco/ [33]	2017	Prospective	70	T2W + DWI + PWI + DTI			94
Abdel Qader Abdel Hameed/ [52]	2018	Retrospective	20	T2WI	62.5	67	63
				DWI	100	100	100
				T2WI + DWI	100	100	100
				Contrast enhanced images	92	100	93
				Contrast enhanced images + DWI	100	100	100
van der Pol/ [6]	2018	Retrospective	45	T2WI + DWI (ADC) + DCE imaging	88–92	74–84	84–86
Barchetti/ [77]	2019	Retrospective	75	T2WI + DWI + DCE imaging	82–91	85–89	

MRI magnetic resonance imaging, *T2WI* T2-weighted imaging, *DWI* diffusion-weighted imaging, *T1WI* T1-weighted imaging, *ADC* apparent diffusion coefficient, *DCE* dynamic contrast enhanced, *DTI* diffusion tensor imaging

bladder cancer, the treatment plan for muscle-invasive bladder cancer was compared before and after PET-CT imaging. Treatment was altered in 20–27% of cases who underwent preoperative PET-CT, mainly due to upstaging by this technique in comparison with conventional imaging [59, 60].

Whether PET-CT is better than CECT in nodal staging is unclear. Some suggest FDG PET-CT is superior with sensitivities ranging from 36 to 78% for PET-CT versus 9.1–44% for CECT [21, 24, 26], others have not [16, 22, 29, 61]. Given the suboptimal performance of PET-CT in the diagnosis of small metastatic lymph nodes, Goodfellow et al. recommended using PET-CT only in patients with either enlarged pelvic LNs and a small primary bladder tumor, in patients with extra pelvic nodal metastases, and in patients who have indeterminate lesions suspicious for metastasis [27]. Although PET-CT showed higher sensitivity for pelvic lymph node detection (68%) compared to PET (46%) or CT (46%) alone, they did not suggest the routine use of PET-CT in the preoperative staging of patients with bladder cancer due to its limited additional value and the high cost.

Non-FDG PET tracers, such as radiolabeled 11C-choline and 11C-acetate have been used to preoperatively assess lymph node involvement of bladder cancer. 11C-acetate and 11C-choline both show increased uptake in neoplastic lesions and since little to no tracer is excreted in the urine, the primary tumor can be seen [62]. Radiolabeled 11C-choline is thought to provide better definition between the tumor and the background compared to

Table 4 MRI characteristics in differentiating organ-confined (≤T2) from non-organ-confined (≥T3) bladder cancer

Author/[Ref]	Year	Study type	Number of patients	MRI sequence	Organ confined vs. non-organ confined		
					Sensitivity (%)	Specificity (%)	Accuracy (%)
Tekes/ [35]	2005	Retrospective	71	Contrast-enhanced images	79–86	79–84	79–85
Watanabe/ [53]	2009	Retrospective	19	T1WI/T2WI	80	79	79
				T1WI/T2WI/contrast enhanced images	80	79	79
				T1WI/T2WI/DWI	40	93	79
Takeuchi/ [40]	2009	Prospective	40	T2WI	50	95	85
				T2WI + DWI	70	97	92
				T2WI + contrast enhanced images	80	92	90
				All sequences	80	97	94
Rajesh/ [48]	2011	Retrospective	100	T2W/contrast-enhanced images	91	60	89
Ghafoori/ [49]	2012	Prospective	86	T1WI/T2W/contrast-enhanced images	93	94	
Wu/ [41]	2013	Prospective	362	T2WI	72–85	85–94	74–92
				DWI	83–88	91–96	90–95
				T2WI + DWI	87–92	94–100	93–99
Gupta/ [44]	2014	Retrospective	60	DCE imaging	90	80	87
				DWI	95	80	90
Rabie/ [42]	2016	Prospective	45	DCE imaging	94	77	84
Zytoon/ [50]	2016	Prospective	50	T2WI	85	94	88
				DWI	100	94	98
				T2WI + DWI	100	94	98
Barsoum/ [39]	2017	Prospective	50	T2WI	92	92	94
				DWI	100	96	98
				T2WI + DWI	100	100	100
Abdel Qader Abdel Hameed/ [52]	2018	Retrospective	20	T2WI	58	50	56
				DWI	100	100	100
				T2WI + DWI	100	100	100
				Contrast enhanced images	90	67	85
				Contrast enhanced images + DWI	100	100	100
van der Pol/ [6]	2018	Retrospective	45	T2WI + DWI (ADC) + DCE imaging	67–72	92	81–83

Table 5 Sensitivity, specificity and accuracy of specific MRI pulse sequences in detecting lymph node involvement in patients with bladder cancer

Author/[Ref]	Year	Study type	Number of patients	MRI sequence	Lymph node metastasis		
					Sensitivity (%)	Specificity (%)	Accuracy (%)
Papalia/ [36]	2011	Prospective	36	DWI (ADC)	76	89	
Daneshmand/ [54]	2012	Prospective	122	DCE imaging	41	91.5	80
Triantafyllou/ [46]	2012	Prospective	75	USPIO	58.3	83	76.4
Birkhäuser/ [47]	2013	Prospective	75	USPIO-DWI	65–75	93–96	
van der Pol/ [6]	2018	Retrospective	45	T2WI + DWI (ADC) + DCE imaging	45	90–93	78–80

acetate, mostly due to the lower background of choline than acetate and not higher uptake of choline [63]. In a study by Picchio et al., 11 C-choline PET demonstrated fewer false positive lymph nodes than did CT [64]. In comparison to 11 C-choline PET-CT for bladder cancer staging, 18F-FDG showed a higher positive predictive value in detecting extravesical lesions (88.2% vs. 79.4%) [65].

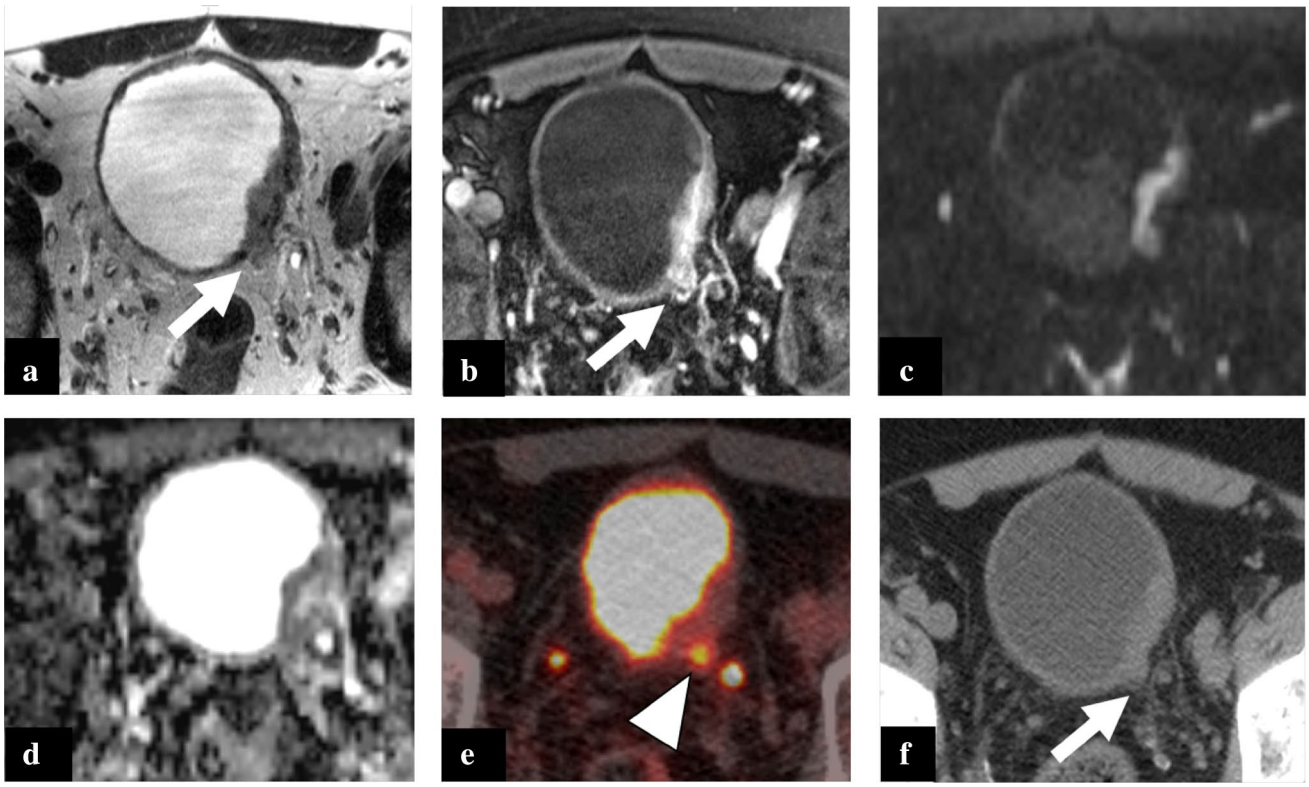

Fig. 7 74-year-old man with left bladder wall mass. There is disruption of the T2 dark detrusor muscle with extension into the perivesical fat (T3) on T2WI (**a**) and DCE (**b**) images (arrows). The mass demonstrates redistricted diffusion with high intensity on high b-value DWI image (**c**) and low signal on corresponding ADC map (**d**). PET-CT (**e**) demonstrates avid uptake of the radiotracer at the site of extravesical extension next to the left ureter (arrowhead). Extravesical extension is also seen on CT (**f**)

The standardized uptake value (SUV) is used to quantitatively assess FDG uptake relative to the background. No specific SUV can be used to differentiate malignant from benign lesions with complete accuracy [16]. In a prospective study of 57 patients with bladder cancers, Apolo et al. reported a sensitivity of 81% and specificity of 94% using a maximum SUV (SUV_{max}) of ≥ 4 for detecting locoregional lymph node involvement [66]. Vind-Kezunovic et al. selected different SUV_{max} cutoff values of 2, 3, 4 and 5 to evaluate the diagnostic ability of FDG PET-CT for detecting lymph node involvement based on SUV_{max}. Their results showed higher specificity at higher values of SUV_{max} (specificity of 91.1% and 97.7% for $SUV_{max} \geq 4$ and $SUV_{max} \geq 5$, respectively) [67].

Hybrid PET-MRI was recently introduced to incorporate the functional information of both MRI and PET with high soft tissue contrast anatomic information of MRI [68]. In a study of 134 patients with pelvic malignancies, Catalano et al. reported that FDG PET-MRI was more accurate than FDG PET-CT in locoregional lymph node staging [69]. Rosenkrantz et al. prospectively analyzed 30 FDG PET-MRI examinations using diuresis protocol in 22 bladder cancer patients. The imaging protocol for this study consisted of injecting FDG one hour prior to imaging followed by forced diuresis. Diuresis was attained by oral hydration and intravenous furosemide. PET-MRI showed higher accuracy (95%) in detecting lymph node involvement as compared to MRI (76%) alone. They suggested a clinically practical role for PET-MRI in the evaluation of patients with bladder cancer especially in clarifying findings that were equivocal on MRI alone [55].

In a recent study of 15 patients with bladder cancer by Salminen et al., the accuracy of PET-MRI in detecting muscle-invasive disease was 73%; the sensitivity, specificity and accuracy for lymph node involvement was 50%, 67% and 60% respectively. Although sensitivity for lymph node involvement was low, the overall accuracy of PET-MRI suggests a potential role for local staging of bladder cancer [70]. Sensitivity, specificity and accuracy of PET-CT and PET-MRI with different techniques and radiotracers for detecting lymph node involvement are shown in Table 6.

Table 6 PET-CT and PET-MRI characteristics for detecting lymph node involvement in patients with bladder cancer

Author/[Ref]	Year	Study type	Number of patients	Imaging modality	Tracer	Lymph node metastasis		
						Sensitivity (%)	Specificity (%)	Accuracy (%)
Drieskens/ [58]	2005	Prospective	55	PET-CT	FDG	60	88	78
				PET	FDG	53	72	65
Kibel/ [71]	2009	Prospective	43	PET-CT	FDG	70	94	88
Swinnen/ [22]	2010	Prospective	51	PET-CT	FDG	46	97	84
Lodde/ [21]	2010	Prospective	70	PET-CT	FDG	57	100	77
Apolo/ [66]	2010	Retrospective	57	PET-CT	FDG	81	94[a]	
Maurer/ [23]	2011	Prospective	44	PET-CT	11C-choline	58	66	64
Schöder/ [72]	2011	Prospective	17	PET-CT	11C-acetate	100	87	
Hitier-Berthsult/ [24]	2012	Prospective	52	PET-CT	FDG	36	87	65
Nayak/ [26]	2013	Prospective	25	PET-CT	FDG	78		
Ceci/ [73]	2014	Retrospective	39	PET-CT	11C-choline	59	90	81
Brunocilla/ [74]	2014	Prospective	26	PET-CT	11C-choline	42	84	73
Goodfellow/ [27]	2014	Retrospective	93	PET	FDG	46	97	82
				PET-CT		68	95	87
Aljabery/ [28]	2015	Retrospective	54	PET-CT	FDG	41	86	
Jeong/ [29]	2015	Prospective	61	PET-CT	FDG	47	93	
Soubra/ [75]	2016	Retrospective	78	PET-CT	FDG	56	98	
Pichler/ [16]	2017	Retrospective	70	PET	FDG	54.5	90	84
				PET-CT	FDG	64[b]	88	84
				PET-CT	FDG	64[c]	86	83
				PET-CT	FDG	73[d]	81	80
Vind-Kezunovic/ [67]	2017	Prospective	119	PET-CT	FDG	78	91[e]	
						65	98[f]	
Salminen/ [70]	2018	Prospective	15	PET-MRI	11C-acetate	50	67	60

PET/CT positron emission tomography/computed tomography, *PET/MRI* positron emission tomography/magnetic resonance imaging, *FDG* fluorodeoxyglucose

[a]At maximum standardized uptake value (SUV_{max}) ≥ 4

[b]Pelvic lymph node is considered positive, if the largest short axis diameter was > 10 mm

[c]Pelvic lymph node is considered positive, if the largest short axis diameter was > 8 mm

[d]Pelvic lymph node involvement was defined based on the subjective assessment

[e]At maximum standardized uptake value (SUV_{max}) ≥ 4

[f]At maximum standardized uptake value (SUV_{max}) ≥ 5

Recent advances and future directions

Standardize reporting

In this article, we presented different perspectives on multiple modalities for the local staging of bladder cancer. Amongst the currently available options to the radiologist, mpMRI has the potential to decrease the inter-observer discrepancy, largely though the depiction of the detrusor muscle and hence whether it is invaded with tumor. In addition to superior soft tissue characterization, the MRI derived functional imaging data that makes this modality to emerge as the locoregional staging imaging method of choice in bladder cancer (Fig. 7). The success of other imaging-based standardized reporting schemes, such as Breast Imaging Reporting and Data System (BI-RADS) and Prostate Imaging Reporting and Data System (PI-RADS) has led to efforts to standardize the MRI reporting in bladder cancer. The fruit of one of these efforts was the publication of the first version of Vesical Imaging-Reporting and Data System (VI-RADS) in 2018 [76]. The authors used the currently available anatomical and function MRI-derived evidence to derive a 5-scale certainty score from highly unlikely (VI-RADS1) to highly likely tumor invasion of muscle and tissues beyond the bladder (VI-RADS5). The four components of the imaging sequences used to establish a VI-RADS score include anatomical imaging with T2WI, and functional imaging using DCE imaging, DWI, and ADC. In this system, priority is given to the T2WI to determine the extent of muscle

involvement; the functional sequences are used to further stratify the mass into VI-RADS categories. This method has been evaluated by Barchetti et al. [77] in 75 patients with bladder cancer. They demonstrated a good interobserver agreement ($k = 0.731$) for accurately categorizing the mass as MIBC versus non-MIBC with AUC of 0.87 and 0.92 between two observers. In a second study using VI-RADS scheme, Wang et al. [78] retrospectively evaluated 340 patients who underwent mpMRI. The area under the ROC curve for muscle invasion was 94% with sensitivity and specificity of 87.1 and 96.5, respectively. Finally, another recent report by Ueno et al. [79] investigated the role of VI-RADS reporting scheme in 74 patients with mpMRI who underwent TURBT. The diagnostic performance of VI-RADS in the differentiation of MIBC vs. non-MIBC was excellent with pooled AUC of 90%. In this study the interclass correlation coefficients (ICC) for interobserver agreements between five radiologists was excellent (ICC: 0.85). Given the excellent diagnostic performance and interobserver agreements of VI-RADS in these preliminary studies, VI-RADS scoring system may eventually become standard way to report pretreatment MRI exams in patients with bladder cancer.

Texture Analysis

There are thousands of pixels in each data set that are presented to the radiologist for interpretation. However, the human eye is capable of recognizing a limited number of shades of gray and associations between adjacent pixels. Texture analysis is a quantitative method for understanding the detailed distributions of pixels or heterogeneity in a given image. Quantitative CT-derived texture analysis has been shown to be associated with tumor grade and survival in patients with colorectal cancer [80], non-small cell lung cancer [81] and esophageal cancer [82] among others. However, given the limitations of CT for tissue characterization in bladder cancer, efforts have been focused on texture analysis of bladder masses using MRI. Recently, Lim et al. [83] investigated the relationship between texture analysis features of the bladder mass and perivesical fat, using T2WI and ADC, in patients who underwent TURBT for staging. Entropy of the mass and extravesical fat were higher for tumors that were stage $\geq$ T3 compared to tumors that were stage $\leq$ T2. Similarly, entropy was higher in the mass and extravesical fat in $\geq$ T2 tumors compared to T1 tumors. Others have shown a similar potential of CT-derived texture analysis in differentiating low-grade versus high-grade urothelial carcinomas [84]. Given the promise of texture analysis in other fields of cancer imaging, one can expect use of higher-order texture analysis for characterization, staging and prognostication of bladder cancer in the future.

Conclusion

Reliable preoperative staging is a critical step in establishing optimal management and treatment decisions in patients with bladder cancer. Extensive efforts are being made to improve the accuracy of both the cross-sectional and molecular imaging modalities in local staging of the bladder cancer. Based on the current evidence, MRI is the modality of choice for locoregional staging of bladder cancer with a combination of anatomic and functional pulse sequences. Despite the advantages of the MRI in the locoregional staging of the bladder cancer, CT urography remains the modality of choice for initial evaluation of patients who present with hematuria. This is mainly due to superior performance of CT in evaluation of the upper urinary tract, in addition to ease of access and convenience for the patients.

Compliance with ethical standards

Conflict of interest The authors declare that they have no conflict of interest.

References

1. Siegel RL, Miller KD, Jemal A (2019) Cancer statistics, 2019. CA: a cancer journal for clinicians 69(1):7-34.
2. National Comprehensive Cancer Network. NCCN Clinical practice guidelines in oncology: bladder cancer. Version 5.2018.
3. van der Pol CB, Sahni VA, Eberhardt SC, Oto A, Akin O, Alexander LF, Allen BC, Coakley FV, Froemming AT, Fulgham PF, Hosseinzadeh K (2018) ACR appropriateness criteria® pretreatment staging of muscle-invasive bladder cancer. Journal of the American College of Radiology 15(5):S150-9.
4. Young FP, Ende D, Epstein RJ (2018) Beyond BCG: the approaching era of personalised bladder-sparing therapies for non-muscle-invasive urothelial cancers. Future Oncology 15(4):409-20.
5. Abdelsalam EM, Adalany MA, Fouda ME (2018) Value of diffusion weighted magnetic resonance imaging in grading of urinary bladder carcinoma. The Egyptian Journal of Radiology and Nuclear Medicine 49(2):509-18.
6. van der Pol CB, Shinagare AB, Tirumani SH, Preston MA, Vangel MG, Silverman SG (2018) Bladder cancer local staging: multiparametric MRI performance following transurethral resection. Abdominal Radiology 43(9):2412-23.
7. Ark JT, Keegan KA, Barocas DA, Morgan TM, Resnick MJ, You C, Cookson MS, Penson DF, Davis R, Clark PE, Smith Jr JA (2014) Incidence and predictors of understaging in patients with clinical T 1 urothelial carcinoma undergoing radical cystectomy. BJU international 113(6):894-9.
8. Amin MB, Edge S, Greene F, Byrd DR, Brookland RK, Washington MK, Gershenwald JE, Compton CC, Hess KR, Sullivan DC, Jessup JM, Brierley JD, Gaspar LE, Schilsky RL, Balch CM, Winchester DP, Asare EA, Madera M, Gress DM, Meyer LR (2017) AJCC Cancer Staging Manual. 8th ed. New York: Springer
9. Hafeez S, Huddart R (2013) Advances in bladder cancer imaging. BMC medicine 11(1):104.

10. Thoeny HC, Froehlich JM, Triantafyllou M, Huesler J, Bains LJ, Vermathen P, Fleischmann A, Studer UE (2014) Metastases in normal-sized pelvic lymph nodes: detection with diffusion-weighted MR imaging. Radiology 273(1):125-35.
11. Bostrom PJ, Van Rhijn BW, Fleshner N, Finelli A, Jewett M, Thoms J, Hanna S, Kuk C, Zlotta AR (2010) Staging and staging errors in bladder cancer. European Urology Supplements 9(1):2-9.
12. Sadow CA, Silverman SG, O'Leary MP, Signorovitch JE (2008) Bladder cancer detection with CT urography in an Academic Medical Center. Radiology 249(1):195-202.
13. Lee CH, Tan CH, Faria SD, Kundra V (2017) Role of imaging in the local staging of urothelial carcinoma of the bladder. American Journal of Roentgenology 208(6):1193-205.
14. Mossanen M, Chang SL, Kimm S, Sonpavde GP, Kibel AS (2018) Current Staging Strategies for Muscle-Invasive Bladder Cancer and Upper Tract Urothelial Cell Carcinoma. The Urologic clinics of North America 45(2):143-54.
15. Caterino M, Giunta S, Finocchi V, Giglio L, Mainiero G, Carpanese L, Crecco M (2001) Primary cancer of the urinary bladder: CT evaluation of the T parameter with different techniques. Abdominal imaging 26(4):433-8.
16. Pichler R, De Zordo T, Fritz J, Kroiss A, Aigner F, Heidegger I, Virgolini I, Horninger W, Uprimny C (2017) Pelvic lymph node staging by combined 18F-FDG-PET-CT imaging in bladder cancer prior to radical cystectomy. Clinical genitourinary cancer 15(3):e387-95.
17. Li Y, Diao F, Shi S, Li K, Zhu W, Wu S, Lin T (2018) Computed tomography and magnetic resonance imaging evaluation of pelvic lymph node metastasis in bladder cancer. Chinese journal of cancer 37(1):3.
18. Schmid SC, Zahel T, Haller B, Horn T, Metzger I, Holzapfel K, Seitz AK, Gschwend JE, Retz M, Maurer T (2016) Prognostic value of computed tomography before radical cystectomy in patients with invasive bladder cancer: imaging predicts survival. World journal of urology 34(4):569-76.
19. Kim JK, Park SY, Ahn HJ, Kim CS, Cho KS (2004) Bladder cancer: analysis of multi–detector row helical CT enhancement pattern and accuracy in tumor detection and perivesical staging. Radiology 231(3):725-31.
20. Baltaci S, Resorlu B, Yagcı C, Turkolmez K, Gogus C, Beduk Y (2008) Computerized tomography for detecting perivesical infiltration and lymph node metastasis in invasive bladder carcinoma. Urologia internationalis 81(4):399-402.
21. Lodde M, Lacombe L, Friede J, Morin F, Saourine A, Fradet Y (2010) Evaluation of fluorodeoxyglucose positron-emission tomography with computed tomography for staging of urothelial carcinoma. BJU international 106(5):658-63.
22. Swinnen G, Maes A, Pottel H, Vanneste A, Billiet I, Lesage K, Werbrouck P (2010) FDG-PET-CT for the preoperative lymph node staging of invasive bladder cancer. European urology 57(4):641-7.
23. Maurer T, Souvatzoglou M, Kübler H, Opercan K, Schmidt S, Herrmann K, Stollfuss J, Weirich G, Haller B, Gschwend JE, Schwaiger M (2012) Diagnostic efficacy of [11C] choline positron emission tomography/computed tomography compared with conventional computed tomography in lymph node staging of patients with bladder cancer prior to radical cystectomy. European urology 61(5):1031-8.
24. Hitier-Berthault M, Ansquer C, Branchereau J, Renaudin K, Bodere F, Bouchot O, Rigaud J (2013) 18 F-fluorodeoxyglucose positron emission tomography–computed tomography for preoperative lymph node staging in patients undergoing radical cystectomy for bladder cancer: A prospective study. International Journal of Urology 20(8):788-96.
25. Tritschler S, Mosler C, Tilki D, Buchner A, Stief C, Graser A (2012) Interobserver variability limits exact preoperative staging by computed tomography in bladder cancer. Urology 79(6):1317-21.
26. Nayak B, Dogra PN, Naswa N, Kumar R (2013) Diuretic 18 F-FDG PET-CT imaging for detection and locoregional staging of urinary bladder cancer: prospective evaluation of a novel technique. European journal of nuclear medicine and molecular imaging 40(3):386-93.
27. Goodfellow H, Viney Z, Hughes P, Rankin S, Rottenberg G, Hughes S, Evison F, Dasgupta P, O'Brien T, Khan MS (2014) Role of fluorodeoxyglucose positron emission tomography (FDG PET)-computed tomography (CT) in the staging of bladder cancer. BJU international 114(3):389-95.
28. Aljabery F, Lindblom G, Skoog S, Shabo I, Olsson H, Rosell J, Jahnson S (2015) PET-CT versus conventional CT for detection of lymph node metastases in patients with locally advanced bladder cancer. BMC urology 15(1):87.
29. Jeong IG, Hong S, You D, Hong JH, Ahn H, Kim CS (2015) FDG PET–CT for lymph node staging of bladder cancer: a prospective study of patients with extended pelvic lymphadenectomy. Annals of surgical oncology 22(9):3150-6.
30. Horn T, Zahel T, Adt N, Schmid SC, Heck MM, Thalgott MK, Hatzichristodoulou G, Haller B, Autenrieth M, Kübler HR, Gschwend JE (2016) Evaluation of computed tomography for lymph node staging in bladder cancer prior to radical cystectomy. Urologia internationalis 96(1):51-6.
31. Oz II, Altinbas NK, Serifoglu I, Oz EB, Yagci C (2016) The role of computerized tomography in the assessment of perivesical invasion in bladder cancer. Polish journal of radiology 81:281.
32. van der Pol CB, Chung A, Lim C, Gandhi N, Tu W, Mclnnes MD, Schieda N (2018) Update on multiparametric MRI of urinary bladder cancer. Journal of Magnetic Resonance Imaging 48(4):882-96.
33. Panebianco V, De Berardinis E, Barchetti G, Simone G, Leonardo C, Grompone MD, Del Monte M, Carano D, Gallucci M, Catto J, Catalano C (2017) An evaluation of morphological and functional multi-parametric MRI sequences in classifying non-muscle and muscle invasive bladder cancer. European radiology 27(9):3759-66.
34. Takeuchi M, Sasaki S, Naiki T, Kawai N, Kohri K, Hara M, Shibamoto Y (2013) MR imaging of urinary bladder cancer for T-staging: A review and a pictorial essay of diffusion-weighted imaging. Journal of Magnetic Resonance Imaging 38(6):1299-309.
35. Tekes A, Kamel I, Imam K, Szarf G, Schoenberg M, Nasir K, Thompson R, Bluemke D (2005) Dynamic MRI of bladder cancer: evaluation of staging accuracy. American Journal of Roentgenology 184(1):121-7.
36. Papalia R, Simone G, Grasso R, Augelli R, Faiella E, Guaglianone S, Cazzato R, Vescovo RD, Ferriero M, Zobel B, Gallucci M (2012) Diffusion-weighted magnetic resonance imaging in patients selected for radical cystectomy: detection rate of pelvic lymph node metastases. BJU international 109(7):1031-6.
37. de Haas RJ, Steyvers MJ, Fütterer JJ (2014) Multiparametric MRI of the bladder: ready for clinical routine?. American Journal of Roentgenology 202(6):1187-95.
38. Sevcenco S, Ponhold L, Heinz-Peer G, Fajkovic H, Haitel A, Susani M, Shariat SF, Szarvas T, Baltzer PA (2014) Prospective evaluation of diffusion-weighted MRI of the bladder as a biomarker for prediction of bladder cancer aggressiveness. InUrologic Oncology: Seminars and Original Investigations (Vol. 32, No. 8, pp. 1166-1171). Elsevier.
39. Barsoum N, Talaat M, Saraya S (2017) Can diffusion-weighted MRI predict the histological grade of urinary bladder carcinoma?. Kasr Al Ainy Medical Journal 23(2):86.
40. Takeuchi M, Sasaki S, Ito M, Okada S, Takahashi S, Kawai T, Suzuki K, Oshima H, Hara M, Shibamoto Y (2009) Urinary bladder cancer: diffusion-weighted MR imaging—accuracy for

diagnosing T stage and estimating histologic grade. Radiology 251(1):112-21.
41. Wu LM, Chen XX, Xu JR, Zhang XF, Suo ST, Yao QY, Fan Y, Hu J (2013) Clinical value of T2-weighted imaging combined with diffusion-weighted imaging in preoperative T staging of urinary bladder cancer: a large-scale, multiobserver prospective study on 3.0-T MRI. Academic radiology 20(8):939-46.
42. Rabie E, Faeghi F, Izadpanahi MH, Dayani MA (2016) Role of dynamic contrast-enhanced magnetic resonance imaging in staging of bladder cancer. Journal of clinical and diagnostic research: JCDR 10(4):TC01.
43. Bagheri MH, Ahlman MA, Lindenberg L, Turkbey B, Lin J, Civelek AC, Malayeri AA, Agarwal PK, Choyke PL, Folio LR, Apolo AB (2017) Advances in medical imaging for the diagnosis and management of common genitourinary cancers. InUrologic Oncology: Seminars and Original Investigations (Vol. 35, No. 7, pp. 473-491). Elsevier.
44. Gupta N, Sureka B, Kumar MM, Malik A, Bhushan TB, Mohanty NK (2015) Comparison of dynamic contrast-enhanced and diffusion weighted magnetic resonance image in staging and grading of carcinoma bladder with histopathological correlation. Urology annals 7(2):199.
45. Sankineni S, Brown AM, Fascelli M, Law YM, Pinto PA, Choyke PL, Turkbey B (2015) Lymph node staging in prostate cancer. Current urology reports 16(5):30.
46. Triantafyllou M, Studer UE, Birkhäuser FD, Fleischmann A, Bains LJ, Petralia G, Christe A, Froehlich JM, Thoeny HC (2013) Ultrasmall superparamagnetic particles of iron oxide allow for the detection of metastases in normal sized pelvic lymph nodes of patients with bladder and/or prostate cancer. European journal of cancer 49(3):616-24.
47. Birkhäuser FD, Studer UE, Froehlich JM, Triantafyllou M, Bains LJ, Petralia G, Vermathen P, Fleischmann A, Thoeny HC (2013) Combined ultrasmall superparamagnetic particles of iron oxide–enhanced and diffusion-weighted magnetic resonance imaging facilitates detection of metastases in normal-sized pelvic lymph nodes of patients with bladder and prostate cancer. European urology 64(6):953-60.
48. Rajesh A, Sokhi HK, Fung R, Mulcahy KA, Bankart MJ (2011) Bladder cancer: evaluation of staging accuracy using dynamic MRI. Clinical radiology 66(12):1140-5.
49. Ghafoori M, Shakiba M, Ghiasi A, Asvadi N, Hosseini K, Alavi M (2013) Value of MRI in local staging of bladder cancer. Urology journal 10(2):866-72.
50. Zytoon AA, Azab SM, Samak WA (2017) Role of magnetic resonance in evaluation of urinary bladder cancer. Menoufia Medical Journal 30(1):104.
51. Lee M, Shin SJ, Oh YT, Jung DC, Cho NH, Choi YD, Park SY (2017) Non-contrast magnetic resonance imaging for bladder cancer: fused high b value diffusion-weighted imaging and T2-weighted imaging helps evaluate depth of invasion. European radiology 27(9):3752-8.
52. Hameed HA, Nagi MA, Wali DH (2018) Role of Diffusion Weighted Magnetic Resonance Imaging (DW-MRI) in Assessment of Urinary Bladder Carcinoma. The Egyptian Journal of Hospital Medicine (July 2018)72(11):5561-70.
53. Watanabe H, Kanematsu M, Kondo H, Goshima S, Tsuge Y, Onozuka M, Moriyama N (2009) Preoperative T staging of urinary bladder cancer: does diffusion-weighted MRI have supplementary value?. American Journal of Roentgenology 192(5):1361-6.
54. Daneshmand S, Ahmadi H, Huynh LN, Dobos N (2012) Preoperative staging of invasive bladder cancer with dynamic gadolinium-enhanced magnetic resonance imaging: results from a prospective study. Urology 80(6):1313-8.
55. Rosenkrantz AB, Friedman KP, Ponzo F, Raad RA, Jackson K, Huang WC, Balar AV (2017) Prospective pilot study to evaluate the incremental value of PET information in patients with bladder cancer undergoing 18F-FDG simultaneous PET-MRI. Clinical nuclear medicine 42(1):e8.
56. Agarwal KK, Roy SG, Kumar R (2016) Diuretic 18F-Fluorodeoxyglucose PET/computed tomography in evaluation of genitourinary malignancies. PET clinics 11(1):39-46.
57. Koyama K, Okamura T, Kawabe J, Ozawa N, Torii K, Umesaki N, Miyama M, Ochi H, Yamada R (2003) Evaluation of 18F-FDG PET with bladder irrigation in patients with uterine and ovarian tumors. Journal of Nuclear Medicine 44(3):353-8.
58. Drieskens O, Oyen R, Van Poppel H, Vankan Y, Flamen P, Mortelmans L (2005) FDG-PET for preoperative staging of bladder cancer. European journal of nuclear medicine and molecular imaging 32(12):1412-7.
59. Mertens LS, Fioole-Bruining A, Vegt E, Vogel WV, van Rhijn BW, Horenblas S (2013) Impact of 18 F-fluorodeoxyglucose (FDG)-positron-emission tomography/computed tomography (PET-CT) on management of patients with carcinoma invading bladder muscle. BJU international 112(6):729-34.
60. Kollberg P, Almquist H, Bläckberg M, Cronberg C, Garpered S, Gudjonsson S, Kleist J, Lyttkens K, Patschan O, Liedberg F(2015) [18 F] Fluorodeoxyglucose–positron emission tomography/computed tomography improves staging in patients with high-risk muscle-invasive bladder cancer scheduled for radical cystectomy. Scandinavian journal of urology 49(4):296-301.
61. Kassem TW. Up and down staging of TCC using 18F-FDG PET-CT scan (2016) The Egyptian Journal of Radiology and Nuclear Medicine 47(3):1095-102.
62. Lee ST, Lawrentschuk N, Scott AM (2012) PET in prostate and bladder tumors. InSeminars in nuclear medicine (Vol. 42, No. 4, pp. 231-246). WB Saunders.
63. Orevi M, Klein M, Mishani E, Chisin R, Freedman N, Gofrit ON (2012) 11C-acetate PET-CT in bladder urothelial carcinoma: intraindividual comparison with 11C-choline. Clinical nuclear medicine 37(4):e67-72.
64. Picchio M, Treiber U, Beer AJ, Metz S, Bössner P, Van Randenborgh H, Paul R, Weirich G, Souvatzoglou M, Hartung R, Schwaiger M (2006) Value of 11C-choline PET and contrast-enhanced CT for staging of bladder cancer: correlation with histopathologic findings. Journal of Nuclear Medicine 47(6):938-44.
65. Golan S, Sopov V, Baniel J, Groshar D (2011) Comparison of 11C-choline with 18F-FDG in positron emission tomography/computerized tomography for staging urothelial carcinoma: a prospective study. The Journal of urology 186(2):436-41.
66. Apolo AB, Riches J, Schöder H, Akin O, Trout A, Milowsky MI, Bajorin DF (2010) Clinical value of fluorine-18 2-fluoro-2-deoxy-D-glucose positron emission tomography/computed tomography in bladder cancer. Journal of Clinical Oncology 28(25):3973.
67. Vind-Kezunovic S, Bouchelouche K, Ipsen P, Høyer S, Bell C, Jensen JB (2017) Detection of lymph node metastasis in patients with bladder cancer using maximum standardised uptake value and 18F-fluorodeoxyglucose positron emission tomography/computed tomography: results from a high-volume centre including long-term follow-up. European urology focus
68. Rosenkrantz AB, Friedman K, Chandarana H, Melsaether A, Moy L, Ding YS, Jhaveri K, Beltran L, Jain R (2016) Current status of hybrid PET-MRI in oncologic imaging. American Journal of Roentgenology 206(1):162-72.
69. Catalano OA, Rosen BR, Sahani DV, Hahn PF, Guimaraes AR, Vangel MG, Nicolai E, Soricelli A, Salvatore M (2013) Clinical impact of PET-MRI imaging in patients with cancer undergoing same-day PET-CT: initial experience in 134 patients—a hypothesis-generating exploratory study. Radiology 269(3):857-69.
70. Salminen A, Jambor I, Merisaari H, Ettala O, Virtanen J, Koskinen I, Veskimae E, Sairanen J, Taimen P, Kemppainen J, Minn H (2018) 11 C-acetate PET-MRI in bladder cancer staging and

treatment response evaluation to neoadjuvant chemotherapy: a prospective multicenter study (ACEBIB trial). Cancer Imaging 18(1):25.
71. Kibel AS, Dehdashti F, Katz MD, Klim AP, Grubb RL, Humphrey PA, Siegel C, Cao D, Gao F, Siegel BA (2009) Prospective study of [18F] fluorodeoxyglucose positron emission tomography/computed tomography for staging of muscle-invasive bladder carcinoma. Journal of Clinical Oncology 27(26):4314.
72. Schöder H, Ong SC, Reuter VE, Cai S, Burnazi E, Dalbagni G, Larson SM, Bochner BH (2012) Initial results with 11 C-acetate positron emission tomography/computed tomography (PET-CT) in the staging of urinary bladder cancer. Molecular Imaging and Biology 14(2):245-51.
73. Ceci F, Bianchi L, Graziani T, Castellucci P, Pultrone C, Eugenio B, Martorana G, Colletti PM, Rubello D, Fanti S, Schiavina R (2015) 11C-choline PET-CT and bladder cancer: lymph node metastasis assessment with pathological specimens as reference standard. Clinical nuclear medicine 40(2):e124-8.
74. Brunocilla E, Ceci F, Schiavina R, Castellucci P, Maffione AM, Cevenini M, Bianchi L, Borghesi M, Giunchi F, Fiorentino M, Chondrogiannis S (2014) Diagnostic accuracy of 11C-choline PET/CT in preoperative lymph node staging of bladder cancer: a systematic comparison with contrast-enhanced CT and histologic findings. Clinical nuclear medicine 39(5):e308-12.
75. Soubra A, Hayward D, Dahm P, Goldfarb R, Froehlich J, Jha G, Konety BR (2016) The diagnostic accuracy of 18F-fluorodeoxyglucose positron emission tomography and computed tomography in staging bladder cancer: a single-institution study and a systematic review with meta-analysis. World journal of urology 34(9):1229-37.
76. Panebianco V, Narumi Y, Altun E, Bochner BH, Efstathiou JA, Hafeez S, Huddart R, Kennish S, Lerner S, Montironi R, Muglia VF (2018) Multiparametric magnetic resonance imaging for bladder cancer: development of VI-RADS (Vesical Imaging-Reporting And Data System). European urology 74(3):294-306.
77. Barchetti G, Simone G, Ceravolo I, Salvo V, Campa R, Del Giudice F, De Berardinis E, Buccilli D, Catalano C, Gallucci M, Catto JW (2019) Multiparametric MRI of the bladder: inter-observer agreement and accuracy with the Vesical Imaging-Reporting and Data System (VI-RADS) at a single reference center. European radiology 1-9.
78. Wang H, Luo C, Zhang F, Guan J, Li S, Yao H, Chen J, Luo J, Chen L, Guo Y (2019) Multiparametric MRI for bladder cancer: validation of VI-RADS for the detection of detrusor muscle invasion. Radiology 182506.
79. Ueno Y, Takeuchi M, Tamada T, Sofue K, Takahashi S, Kamishima Y, Hinata N, Harada K, Fujisawa M, Murakami T (2019) Diagnostic Accuracy and Interobserver Agreement for the Vesical Imaging-Reporting and Data System for Muscle-invasive Bladder Cancer: A Multireader Validation Study. European Urology.
80. Ng F, Ganeshan B, Kozarski R, Miles KA, Goh V (2013) Assessment of primary colorectal cancer heterogeneity by using whole-tumor texture analysis: contrast-enhanced CT texture as a biomarker of 5-year survival. Radiology 266(1):177-84.
81. Ganeshan B, Abaleke S, Young RC, Chatwin CR, Miles KA (2010) Texture analysis of non-small cell lung cancer on unenhanced computed tomography: initial evidence for a relationship with tumour glucose metabolism and stage. Cancer imaging 10(1):137.
82. Ganeshan B, Skogen K, Pressney I, Coutroubis D, Miles K (2012) Tumour heterogeneity in oesophageal cancer assessed by CT texture analysis: preliminary evidence of an association with tumour metabolism, stage, and survival. Clinical radiology 67(2):157-64.
83. Lim CS, Tirumani S, van der Pol CB, Alessandrino F, Sonpavde GP, Silverman SG, Shinagare AB (2019) Use of Quantitative T2-Weighted and Apparent Diffusion Coefficient Texture Features of Bladder Cancer and Extravesical Fat for Local Tumor Staging After Transurethral Resection. American Journal of Roentgenology 1-0.
84. Sun H, Shi B, Jin ZY, Xue HD (2017). Quantitative CT texture analysis for evaluating histologic grade of urothelial carcinoma. Abdominal Radiology 42(2): 561-8.